

Selected Papers

Preparation and Structural Features of Cu(I)Cu(II) Coordination Polymers Obtained by Using Tripodal Complexes as Bridging Ligands

Yuki Yoshida,[1] Riichi Miyamoto,[1] Ayami Nakato,[1,4] Ryoko Santo,[1] Naoto Kuwamura,[1,3,4] Kenji Gobo,[1] Takanori Nishioka,*[1,3] Masakazu Hirotsu,[1] Akio Ichimura,[1] Hideki Hashimoto,[2,3,4] and Isamu Kinoshita*[1,3,4]

[1]Department of Chemistry, Graduate School of Science, Osaka City University, 3-3-138 Sugimoto, Sumiyoshi-ku, Osaka 558-8585

[2]Department of Physics, Graduate School of Science, Osaka City University, 3-3-138 Sugimoto, Sumiyoshi-ku, Osaka 558-8585

[3]CREST, Japan Science and Technology Agency, 4-1-8 Honcho, Kawaguchi, Saitama 332-0012

[4]The OCU Advanced Research Institute for Natural Science and Technology (OCARINA), Osaka City University, 3-3-138 Sugimoto, Sumiyoshi-ku, Osaka 558-8585

Received December 27, 2010; E-mail: nishioka@sci.osaka-cu.ac.jp

A tripodal complex [CuCl(tpmtm)] (tpmtm: tris(2-pyrimidylthio)methanide) is used to synthesize coordination polymers. The tripodal complex unit worked as bidentate, tridentate, or tetradentate bridging ligands for $[Cu_nCl_m]$ units via coordination of three outer nitrogen atoms of the tpmtm ligand and also an axial chloro ligand. X-ray crystallography exhibited that obtained coordination polymers contained novel structures of $[Cu_nCl_m]$ moieties such as chloride-bridged linear $Cu^ICu^{II}Cu^I$ and $Cu^ICu^{II}Cu^{II}Cu^I$ and cage-shaped $Cu^ICu^{II}Cu^{II}Cu^I$ mixed-valence copper cluster units. The relationship between the numbers of the outer coordination sites on the tripodal complex and structures of the coordination polymers is observed showing that participation in the coordination of two, three, or four outer coordination sites on the tripodal complex afforded the one-dimensional chain, two-dimensional sheet, or three-dimensional structures, respectively.

A considerable number of coordination polymers have attracted much attention concerning zeolite alternatives,[1] semiconductors,[2] and proton-conductors,[3] and the related field of coordination space has been fully developed.

Coordination polymers have been designed to regulate structure by choosing and developing appropriate organic ligands suitable for particular systems. The control of the dimension of coordination polymers is an especially important factor for the construction of the polymer system. Many coordination polymer systems with such structural regulation provide interesting properties.[4]

We have found that a tripod ligand, tris(2-pyridylthio)-methanide (tptm) (Scheme 1), coordinates to a metal ion, such as Cu to form trigonal bipyramidal complex, $[Cu^{II}L(tptm)]^{n+}$ ($L = CH_3CN$, halides, OH, OH_2).[5–10] These copper complexes exhibit well reversible redox processes for Cu^{III}/Cu^{II} conversion with almost no structural changes around the coordination sphere of the central copper ion. Replacement of the pyridine rings in the tptm ligand with pyrimidine rings forms tetradentate tripodal ligand, tris(2-pyrimidylthio)methanide (tpmtm), which presumably coordinates to a copper ion through the carbanion carbon and three nitrogen atoms and also contains three additional nitrogen atoms capable of forming coordination linkages meaning that the proposed complexes, $[CuX(tpmtm)]^{0/+}$ can act as a bridging unit. Furthermore, when a halogen atom coordinates to the copper ion of the tpmtm complex as an axial ligand, the halogen ligand possibly works as a bridging ligand, then the trigonal bipyramidal tpmtm complexes work as a tetradentate bridging ligand (Scheme 2). As a whole, these properties and structural character bring the ability to control dimensionality and valence states of polymers. Furthermore, the tpmtm complexes can be utilized as redox active building blocks to develop

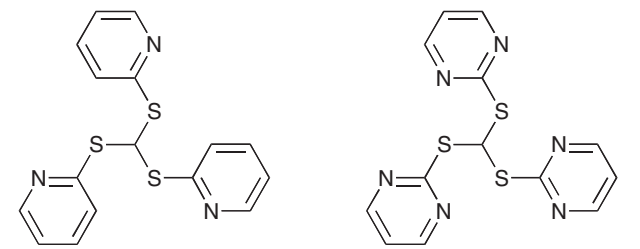

Scheme 1.

Published on the web June 4, 2011; doi:10.1246/bcsj.20100361

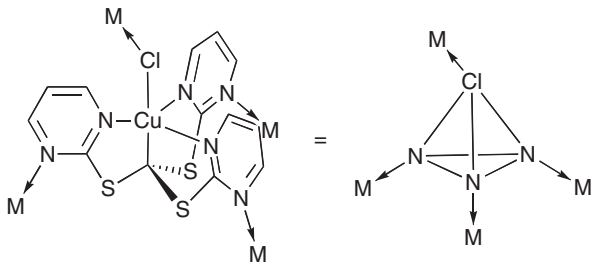

Scheme 2.

mixed-valence coordination polymers, which show interesting properties such as electric conductivity.

We have tried to prepare a mixed-valence coordination polymer containing copper(II) and copper(III) tpmtm complexes using [CuCl(tpmtm)] in the presence of a variety of oxidizing agents and in the course of the trials, we obtained coordination polymers containing [$Cu^{II}Cl$(tpmtm)] units with the novel structures of [Cu_nCl_m] moieties as bridging units. X-ray structural analyses of the coordination polymers revealed a relationship between the number of the outer coordination sites in the [CuCl(tpmtm)] building block.

Results and Discussion

Cu(II) tpmtm Complexes. A tripod ligand precursor, tris(2-pyrimidylthio)methane (tpmtmH), and its copper(II) chloro complex, [CuCl(tpmtm)], were synthesized in similar manner to those of tptmH and its copper(II) complex. The acetonitrile complex **1** was prepared by the reaction of tpmtmH and [$Cu(CH_3CN)_4$](PF_6) in a mixed solvent (CH_2Cl_2:CH_3CN = 10:1) under aerobic conditions. Addition of a small amount of water to a solution of the acetonitrile complex in acetone gave the aqua complex, $[Cu(OH_2)(tpmtm)]^+$, which easily converted to the chloro complex by reaction with a source of chloride such as sodium chloride. The hydroxo complex, [Cu(OH)(tpmtm)](Et_3NH)(PF_6) (**2**), was obtained by the reaction of [$Cu(CH_3CN)_4$](PF_6) and tpmtmH in dichloromethane in the presence of triethylamine under aerobic conditions possibly passing through a peroxo species.

The structures of [$Cu(CH_3CN)$(tpmtm)](PF_6) (**1**), [Cu(OH)-(tpmtm)](Et_3NH)(PF_6) (**2**), and [CuCl(tpmtm)] (**3**) were analyzed by X-ray crystallography (Figures 1–3 and Table 1). The framework of the cationic moiety of each tpmtm complex is similar to the corresponding tptm complex. However, the coordination geometry around the metal center of the tpmtm complexes are more distorted toward square pyramidal from trigonal bipyramidal compared with those of the tptm complexes, which have trigonal bipyramidal structures. These distortions between square pyramidal and trigonal bipyramidal geometries clearly appeared in τ values, which can be calculated by $\tau = \{$(the largest L–M–L angle) − (the second largest L–M–L angle)$\}/60$ giving 0.0 and 1.0 for the ideal square pyramidal and trigonal bipyramidal geometries, respectively.[11] The tptm complexes exhibit trigonal bipyramidal coordination geometry ($\tau = 1.01$ for X = OH; 0.97 for CH_3CN; 0.85(av) for Cl), especially for the tpmtm hydroxo complex, which shows very distorted coordination geometry toward square pyramidal ($\tau = 0.42$ for X = OH; 0.71 for CH_3CN; 0.65 for Cl). This larger distortion of the tpmtm hydroxo complex is attributed to the orientation of the triethylammonium ion, which is bound to the hydroxo ligand via hydrogen bonding. In the case of the tptm hydroxo complex, the N–H bond of the triethylammonium ion is located on the crystallographic C_3 axis, which also contains the oxygen of the hydroxo group, copper, and carbanion carbon atoms. On the other hand, the triethylammonium ion in the crystal of the tpmtm hydroxo complex tilted toward the basal plane made of two pyridine nitrogens, oxygen of the hydroxo group, and carbanion carbon atoms, probably due to the distorted square

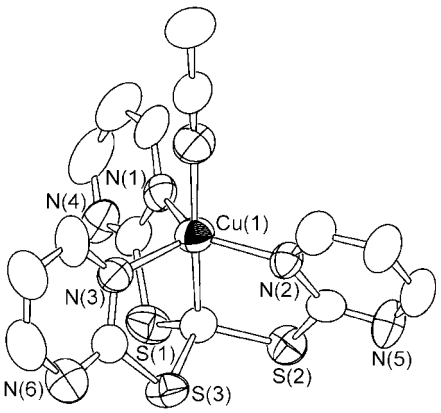

Figure 1. Structure of cationic moiety of [$Cu(CH_3CN)$(tpmtm)](PF_6) (**1**).

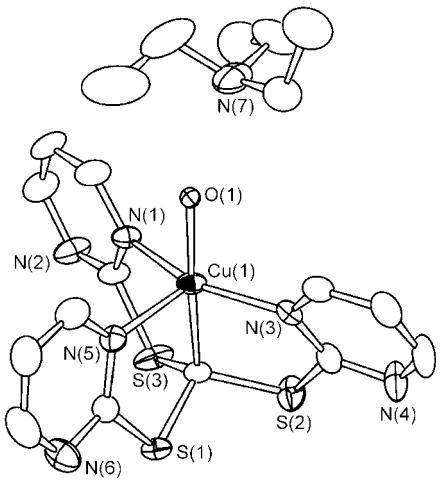

Figure 2. Structure of molecular copper complex and Et_3NH^+ in [Cu(OH)(tpmtm)](Et_3NH)(PF_6) (**2**).

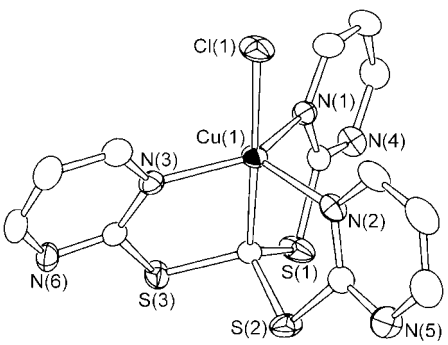

Figure 3. Structure of [CuCl(tpmtm)] (**3**).

Table 1. Comparison of Selected Bond Distances (Å) and Angles (°) and τ Parameters of Cu tpmtm and tptm Complexes

	Complexes					
	$[Cu(CH_3CN)(L)](PF_6)$		$[Cu(OH)(L)](Et_3NH)(PF_6)$		[CuCl(L)]	
L:	tpmtm (**1**)	tptm	tpmtm (**2**)	tptm	tpmtm (**3**)	tptm (av)
Cu–C	2.000(8)	2.004(3)	2.024(4)	2.012(7)	2.0363(19)	2.013(8)
Cu–X_{ax}	2.027(8)	2.028(3)	1.929(2)	1.933(4)	2.2907(6)	2.315(5)
Cu–N	2.011(8)	2.074(3)	2.022(3)	2.088(3)	2.0771(17)	2.080(7)
	2.038(8)	2.077(3)	2.013(3)		2.0934(16)	2.099(7)
	2.088(7)	2.084(3)	2.152(2)		2.1526(17)	2.133(9)
C–Cu–X_{ax}	178.1(3)	179.7(1)	177.47(11)	180	178.52(5)	178.2(6)
N–Cu–N	111.5(3)	116.6(1)	100.90(12)	119.68(2)	109.09(6)	109(3)
	112.3(3)	120.7(1)	106.17(12)		110.32(6)	122.1(12)
	135.3(3)	121.5(1)	152.35(12)		139.27(6)	127(3)
τ	0.71	0.97	0.42	1.01	0.65	0.85

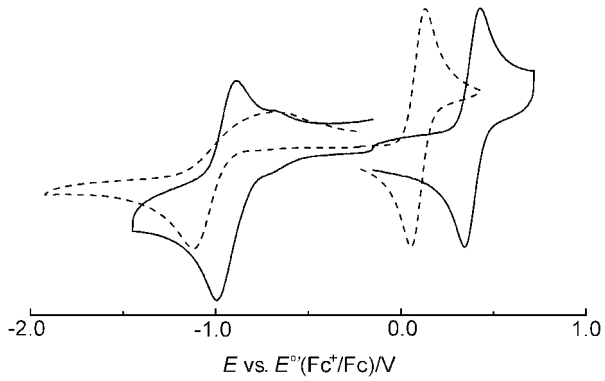

Figure 4. Cyclic voltammograms of [CuCl(tpmtm)] (solid line) and [CuCl(tptm)] (dashed line).

pyramidal coordination geometry of the tpmtm complex. In dichloromethane, the hydroxo complex **2** showed a similar UV–vis spectrum with that of the tptm copper fluoride complex [CuF(tptm)], which retains its trigonal bipyramidal structure in solution. In addition, the cyclic voltammogram of **2** also exhibit a similar redox behavior to those of the tptm complexes with halide as an apical ligand and [CuCl(tpmtm)]. The similarity of absorption and voltammetric properties strongly indicates that the hydroxo complex **2** has a trigonal bipyramidal structure in solution, probably due to the release of the triethylammonium ion bound to the hydroxo ligand in the solid state.

Cyclic voltammetry of [CuCl(tpmtm)] (**3**) exhibited reversible oxidation at ca. 380 mV (vs. $E^{0'}(Fc^{+/0})$) which is ca. 340 mV higher than the corresponding tptm chloro complex (Figure 4). This is attributed to the stabilization of the copper(II) state mainly due to the electron-withdrawing effect of the pyrimidine moieties lowering the energy level of the d_{z^2} orbital.

Coordination Polymers. $[\{CuCl(tpmtm)\}_2(Cu_2Cl_2)]_n \cdot 2nC_4H_8O_2$ (P1) and $[\{CuCl(tpmtm)\}_2(Cu_2Cl_2)]_n \cdot n[CuCl(tpmtm)]$ (P2): A coordination polymer **P1** was obtained as single crystals from a mixture of [CuCl(tpmtm)] (**3**), CuCl, and KPF_6 in 1,4-dioxane by slow diffusion of hexane. X-ray crystallographic analysis showed that **P1** consists of the $[Cu^{II}Cl(tpmtm)]$ and $[Cu^{I}_2Cl_2]$ units in 2:1 ratio (Figure 5). There are two crystallographically independent coordination

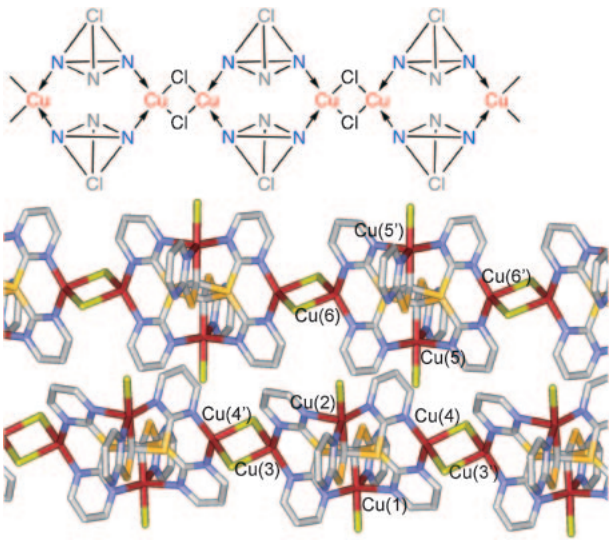

Figure 5. Schematic description (top) and crystallographically independent polymer chains (bottom) of $[\{CuCl(tpmtm)\}_2(Cu_2Cl_2)]_n$ in **P1**.

polymer chains, which are similar to each other, in the crystal of **P1**. Two $[Cu^{II}Cl(tpmtm)]$ units bridge in between every two $[Cu^{I}_2Cl_2]$ moieties to form a one-dimensional coordination polymer.

Single crystals of **P2** were obtained by slow evaporation of the solvent of a mixture of [CuCl(tpmtm)] (**3**), $CuCl_2$, and $[Cu(CH_3CN)_4](PF_6)$. Crystals of **P2** contain not only similar one-dimensional coordination polymer chains as **P1** but also discrete molecules of [CuCl(tpmtm)] (**3**) (Figure 6). The $[Cu^{I}_2Cl_2]$ units in both **P1** and **P2** have similar framework found in other Cu(I) dimers with pyridine derivative ligands such as $[\{Cu(2\text{-Mepy})_2\}_2(\mu\text{-Cl})_2]$ (2-Mepy: 2-picoline)[12,13] and $[\{Cu(2,4\text{-Me}_2py)_2\}_2(\mu\text{-Cl})_2]$ (2,4-Me$_2$py: 2,4-dimethylpyridine).[13] The Cl–Cu–Cl bond angles in **P1** and **P2** (95.97(11)–97.35(10)° for **P1** and 98.07(16)° for **P2**) are smaller than those found in the pyridine complexes (100.07(5) and 105.31(3)° for 2-picoline and 2,4-dimethylpyridine complexes, respectively), while the Cu–Cl–Cu bond angles in **P1** and **P2** (82.32(10)–85.22(12) and 81.93(18)°) are larger than those found in the pyridine complexes (Table 2).

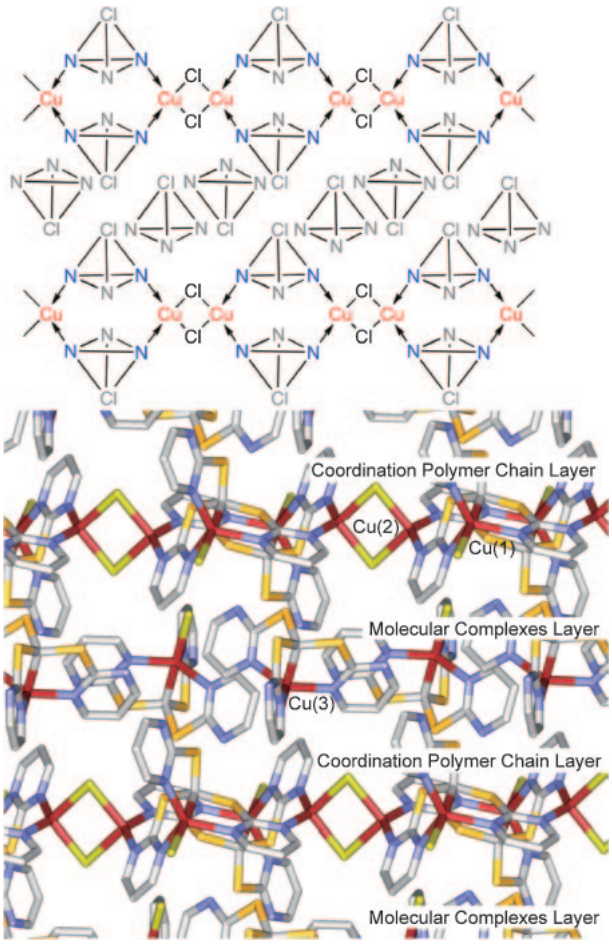

Figure 6. Schematic description (top) and crystal packing of $[\{CuCl(tpmtm)\}_2(Cu_2Cl_2)]_n \cdot n[CuCl(tpmtm)]$ (bottom) in **P2**.

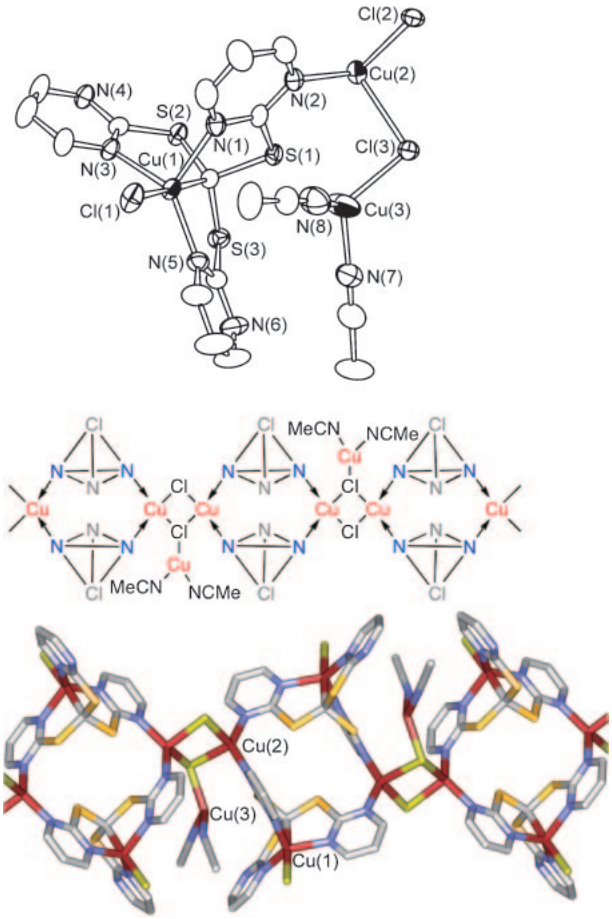

Figure 7. Asymmetric unit (top), schematic description (middle), and polymer structure (bottom) of $[\{CuCl(tpmtm)\}_2(Cu_2Cl_2\{Cu(CH_3CN)_2\})]_n$ in **P3** (one of the disordered $[Cu(CH_3CN)_2]$ units occurred by the symmetry operation are omitted for clarity).

Table 2. Selected Bond Distances (Å) and Angles (°) for $[Cu_2Cl_2]$ Units in Coordination Polymers

	P1	**P2**	**P3**	**P4**	**P7**
Cu–Cl	2.354(4)–2.464(2)	2.395(4), 2.447(5)	2.3849(15), 2.4796(16)	2.3744(16)–2.4665(15)	2.3106(18)–2.4775(14)
Cu–N	1.956(7)–2.005(7)	1.990(14), 2.016(14)	1.979(3), 1.998(3)	1.978(4)–1.999(4)	1.993(5)–2.041(4)
Cl–Cu–Cl	95.97(11)–97.35(10)	98.07(16)	94.86(5)	95.89(5), 96.06(5)	98.24(5), 99.08(6)
N–Cu–N	130.3(3)–133.0(3)	131.3(5)	132.11(16)	129.73(13), 131.79(19)	126.35(19)
(N–Cu–Cl)					(113.90(15))
Cu–Cl–Cu	82.32(10)–85.22(12)	81.93(18)	81.55(6), 85.54(6)	80.66(4), 83.86(5)	80.92(6), 81.76(5)

$[\{CuCl(tpmtm)\}_2(Cu_2Cl_2\{Cu(CH_3CN)_2\})]_n(PF_6)_n \cdot n$PhMe$\cdot n$$CH_3CN$ (P3) and $[\{CuCl(tpmtm)\}_2(Cu_2Cl_2\{Cu(CH_3CN)_2\})]_n(PF_6)_n \cdot 1.3n$$Et_2O \cdot 0.6n$$CH_3CN$ (P4): Crystals of **P3** and **P4** contain very similar one-dimensional coordination polymers, which consist of the one-dimensional polymer chains found in **P1** or **P2** and additional $[Cu^I(CH_3CN)_2]$ units coordinated by the bridging chloro ligand. Differences between **P3** and **P4** are the solvents for crystallization and coordination environments around the copper center of the $[Cu^I(CH_3CN)_2]$ units. In **P4**, the copper center of the $[Cu^I(CH_3CN)_2]$ units coordinated by two nitrogen atoms of the acetonitrile ligands and a sulfur atom of the neighboring $[Cu^{II}Cl(tpmtm)]$ unit (Cu–S: 2.587(2) Å), while the copper center of the $[Cu^I(CH_3CN)_2]$ units in **P3** coordinated by only acetonitrile nitrogen atoms (Cu···S: 2.711(3) Å) (Figures 7 and 8).

The structures of the $[Cu^I_2Cl_2]$ moieties in **P3** and **P4** are comparable to those in **P1** and **P2** with slightly elongated Cu–Cl bonds attributed to the coordination of one of the bridging chloro ligands to the additional copper center of the $[Cu^I(CH_3CN)_2]$ unit.

$[\{CuCl(tpmtm)\}_2(Cu_4Cl_6)]_n \cdot 4n$$CH_2Cl_2$ (P5): Crystals of **P5** were obtained by standing a reaction mixture of [CuCl(tpmtm)] (**3**) and $(p\text{-}BrC_6H_4)_3NPF_6$ after addition of a mixture of CuCl and Bu_4NCl for 2 weeks. X-ray crystallographic

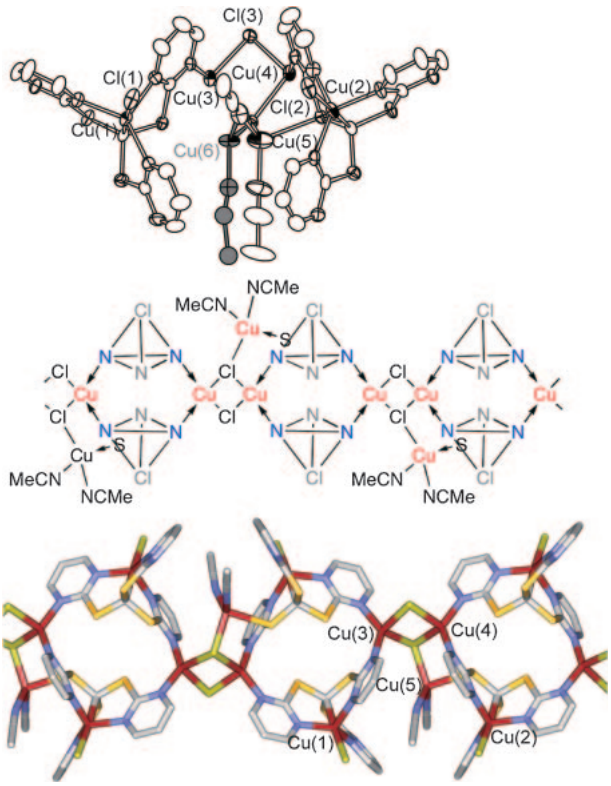

Figure 8. Asymmetric unit with disordered [Cu(CH_3CN)] unit indicated by gray color (top), schematic description (middle), and polymer structure (bottom) of [{CuCl(tpmtm)}$_2$(Cu_2Cl_2{Cu(CH_3CN)$_2$})]$_n$ in **P4** (disordered [Cu(CH_3CN)$_2$] units with smaller occupancies are omitted for clarity).

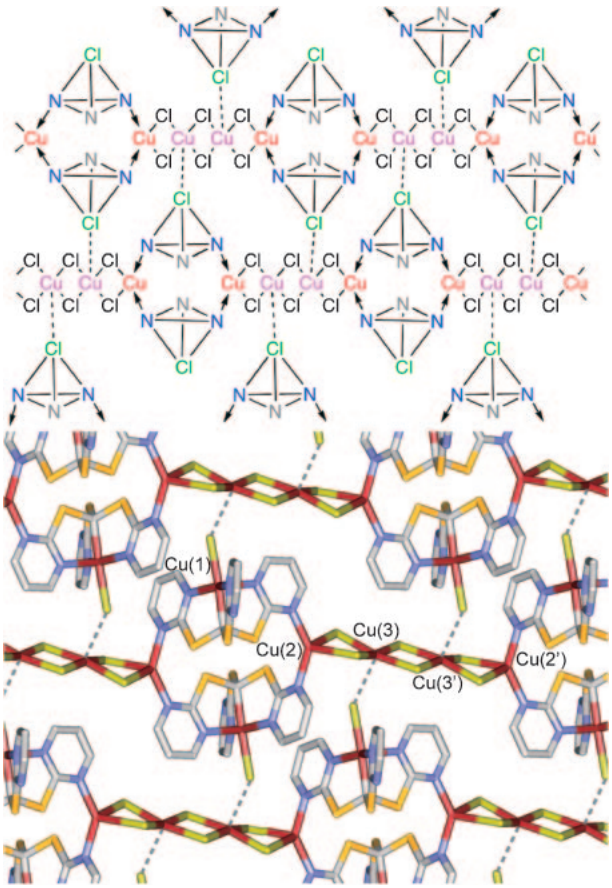

Figure 9. Schematic description (top) and polymer structure (bottom) of [{CuCl(tpmtm)}$_2$(Cu_4Cl_6)]$_n$ in **P5**.

analysis of **P5** exhibited that it contains one-dimensional coordination polymer chains similar to those found in **P1** and **P2** but the [Cu^{II}Cl(tpmtm)] units bridge [Cu_4Cl_6] units instead of the [$Cu^{I}_2Cl_2$] units (Figure 9). The central two of four copper ions in the neutral [Cu_4Cl_6] unit adopt slightly distorted square planar coordination geometry suggesting the oxidation states of +II of the central two copper ions. The Cu–Cl bonds for the two central copper ions (2.2533(9)–2.3062(9) Å) are significantly shorter than those for the two terminal copper ions of the [Cu_4Cl_6] units (2.4911(9) and 2.4947(9) Å). This fact also supported the oxidation states of +II for the central two and +I for terminal two copper ions of the [Cu_4Cl_6] unit. The intention of making the coordination polymer with [Cu^{III}Cl(tpmtm)]$^+$ afforded this linear chain polymer in **P5** as a result. The formation of the polymer in **P5** includes the oxidation of [$Cu^{I}Cl_2$]$^-$ by some oxidants, such as (p-BrC_6H_4)$_3$$NPF_6$ or [Cu^{III}Cl(tpmtm)]$^+$, to provide the [$Cu^{II}Cl_2$] units. This [Cu_4Cl_6] unit is the first example for the halide-bridged linear mixed-valence $Cu^{I}Cu^{II}Cu^{II}Cu^{I}$ tetranuclear unit. The shortest distance between the axial chloro ligand in the [Cu^{II}Cl(tpmtm)] unit and one of the two central copper ions in the [Cu_4Cl_6] unit is 2.7704(8) Å implying a weak interaction between them (dashed lines in Figure 9). When this interaction is included as a coordination bond, the coordination polymer presumably has two-dimensional sheet structure.

[{CuCl(tpmtm)}$_2$(Cu_3Cl_4)]$_n$[{CuCl(tpmtm)}$_2$(Cu_4Cl_6)]$_n$·4$n$$CH_3CN$ (P6): Crystals of **P6** were obtained from a reaction mixture of [CuCl(tpmtm)] (**3**), $CuCl_2$, and $AgPF_6$. Crystallographic analysis of **P6** showed that there are two kinds of coordination polymers in the crystal (Figure 10). One of them is a one-dimensional coordination chain similar to that found in **P5** but the [Cu^{II}Cl(tpmtm)] complexes bridge [Cu_3Cl_4] mixed-valence units instead of the linear [Cu_4Cl_6] units (Figure 11). Central copper ion in the neutral [Cu_3Cl_4] unit adopt square planar coordination geometry and Cu–Cl bond distances around the central copper ion (2.3061(11)–2.3101(12) Å) are significantly shorter than those around the terminal copper ions (2.4550(13) and 2.4580(13) Å) which is consistent with the oxidation states of +II of the central copper ion (Table 3). This [Cu_3Cl_4] unit is also the first example for the halide-bridged linear mixed-valence $Cu^{I}Cu^{II}Cu^{I}$ trinuclear unit. The distances between the axial chloro ligands of the [Cu^{II}Cl(tpmtm)] units in the two neighboring polymer chains and the central copper ion in the [Cu_3Cl_4] unit are 2.9201(15) Å implying very weak interactions between them. When these interactions are included as coordination bonds, the coordination geometry of the central copper ion become axial elongated octahedral and the coordination polymer presumably have two-dimensional sheet structure.

Another coordination polymer in **P6** consists of [CuCl(tpmtm)] and cage-shaped [Cu_4Cl_6] units in a 2:1 ratio (Figure 12). In this coordination polymer, all three outer

nitrogen atoms of the tpmtm ligand in [$Cu^{II}Cl$(tpmtm)] units participated in the coordination with chloride-bridged copper cluster units. The chloride-bridged tetranuclear copper cluster unit adopts a cage-like shape in which each of two [$Cu^{I}Cl_2$] units for Cu(4) and Cu(4′) bridges two copper ions in a [$Cu^{II}{}_2Cl_2$] dimeric unit for Cu(3) and Cu(3′) as shown in Figure 13. The copper ions in the [$Cu^{II}{}_2Cl_2$] dimeric unit adopt distorted square pyramidal geometry with $\tau = 0.33$. The Cu–Cl bond distances for the copper center in the [$Cu^{II}{}_2Cl_2$] dimeric unit (2.2647(13)–2.2942(13) Å) are significantly shorter than those for the [$Cu^{I}Cl_2$] bridging units (2.4192(15) and 2.5264(15) Å) except for the axial Cu–Cl bond for the square pyramidal complex moiety (2.5782(17) Å) exhibiting the oxidation states of the copper ions of +II for the dimeric unit and +I for the bridging units. Noteworthy, the cage-shaped structure found in **P6** is the first example for halide-bridged copper cluster units.

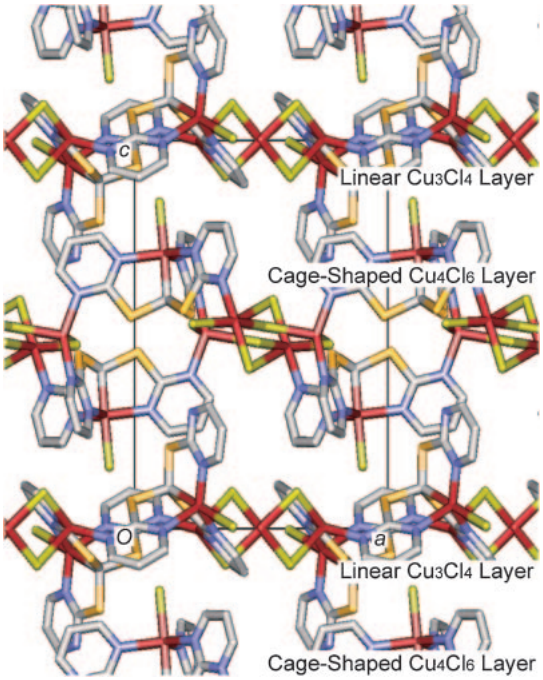

Figure 10. Crystal packing of [{CuCl(tpmtm)}$_2$(Cu_3Cl_4)]$_n$-[{CuCl(tpmtm)}$_2$(Cu_4Cl_6)]$_n$ in **P6**.

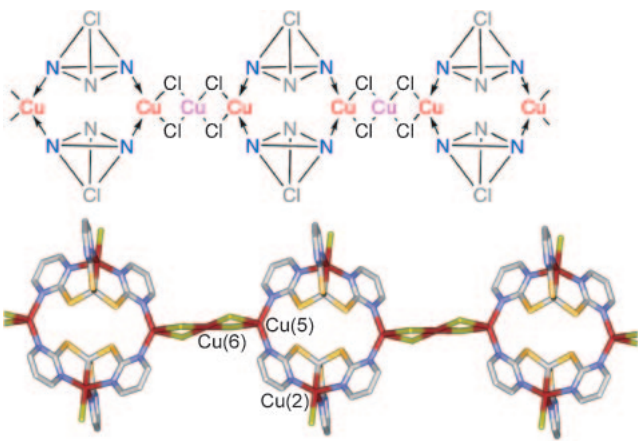

Figure 11. Schematic description (top) and linear chain structure (bottom) of [{CuCl(tpmtm)}$_2$(Cu_3Cl_4)]$_n$ in **P6**.

[{CuCl(tpmtm)}(Cu_2Cl_2)]$_n$·$n$$CH_2Cl_2$ (P7): Crystals of **P7** were obtained from a reaction mixture of [CuCl(tpmtm)] (**3**)

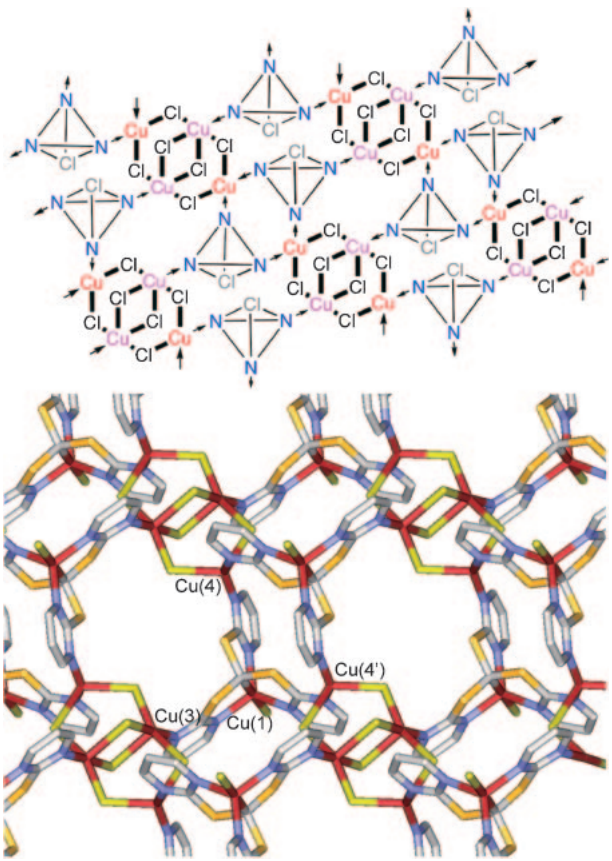

Figure 12. Schematic description (top) and two-dimensional sheet structure (bottom) of [{CuCl(tpmtm)}$_2$-(Cu_4Cl_6)]$_n$ in **P6**.

Table 3. Selected Bond Distances (Å) for Copper Chloride Cluster Units in Coordination Polymers

	Linear [Cu_4Cl_6] in **P5**		Linear [Cu_3Cl_4] in **P6**		Cage-shaped [Cu_4Cl_6] in **P6**	
	Cu(2) (Cu(I))	Cu(3) (Cu(II))	Cu(5) (Cu(I))	Cu(6) (Cu(II))	Cu(3) (Cu(II))	Cu(4) (Cu(I))
Cu–Cl	2.4911(9)	2.2533(9)	2.4550(13)	2.3061(11)	2.2647(13)	2.4192(15)
	2.4947(9)	2.2881(8)	2.4580(13)	2.3101(12)	2.2824(14)	2.5264(15)
		2.2901(9)			2.2942(13)	
		2.3062(9)			2.5782(17)	
Cu–N	1.976(2)		1.992(4)		2.067(4)	1.991(4)
	1.981(2)		1.992(4)			1.998(4)

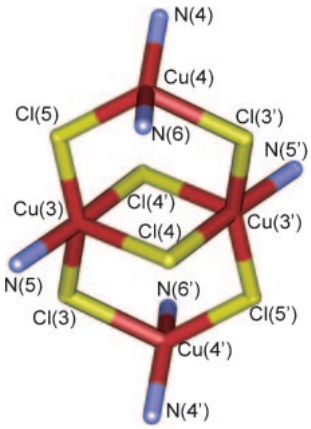

Figure 13. Structure of cage-shaped $[Cu_4Cl_6]$ core in **P6**.

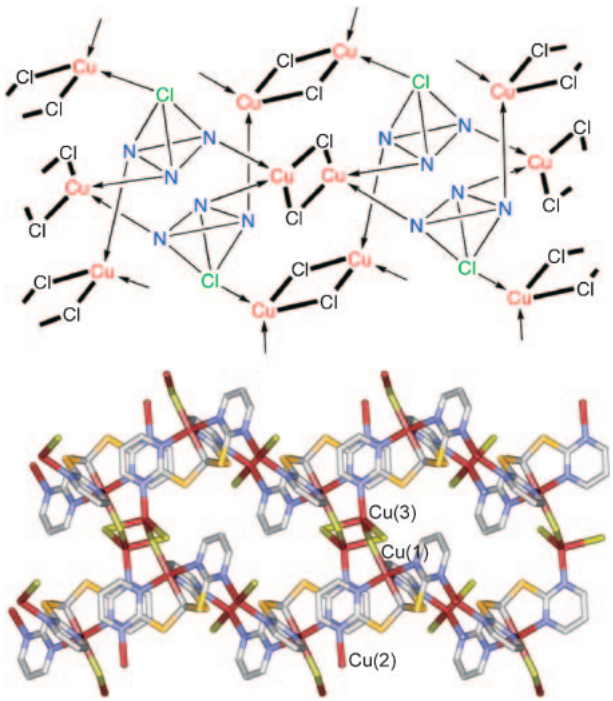

Figure 14. Schematic description (top) and three-dimensional structure (bottom) of $[\{CuCl(tpmtm)\}(Cu_2Cl_2)]_n$ in **P7**.

and $[Cu(CH_3CN)_4](PF_6)$ by standing for 2 weeks. The polymer contained more chloride ions than expected from the amount of the starting materials and the yield. Abstraction of chlorides from dichloromethane molecules, used for solvent, probably occurred during the formation of **P7**.

In **P7**, a $[Cu^{II}Cl(tpmtm)]$ unit is bridged with other four surrounding $[Cu^{II}Cl(tpmtm)]$ moieties by four copper ions in individual $[Cu^{I}_2Cl_2]$ units to form a three-dimensional coordination polymer (Figure 14). All four coordination sites of a $[Cu^{II}Cl(tpmtm)]$ complex moiety, including three outer nitrogen atoms of tpmtm and an axial chloro ligand, participate in coordination to four individual $[Cu^{I}_2Cl_2]$ units. There are two kinds of $[Cu^{I}_2Cl_2]$ units. One of them is to connected four individual $[Cu^{II}Cl(tpmtm)]$ moieties via coordination bonds between the copper ion and one of three outer nitrogen atoms in each tpmtm ligand. Another unit also bridges four individual $[Cu^{II}Cl(tpmtm)]$ moieties but each of two copper ions in the $[Cu^{I}_2Cl_2]$ unit is coordinated by one of three outer nitrogen atoms in one $[Cu^{II}Cl(tpmtm)]$ moiety and the axial chloro ligand of another $[Cu^{II}Cl(tpmtm)]$ moiety. The structure of the $[Cu^{I}_2Cl_2]$ framework of both units is comparable to those found in the other coordination polymers containing $[Cu^{II}Cl(tpmtm)]$.

Structural Features of [CuCl(tpmtm)] Moieties in Coordination Polymers. The $[Cu^{II}Cl(tpmtm)]$ moiety acts as a pseudo-tetrahedral bridging ligand via three outer nitrogen atoms and an axial chloro ligand. The longest Cu–Cl bond in the $[Cu^{II}Cl(tpmtm)]$ moiety (2.3235(13) Å) is observed for three-dimensional polymer in **P7**, in which the axial chloro ligand participated in the coordination to another copper ion. In this point of view that additional coordination of the axial chloro ligand causes elongation of the Cu–Cl bond, the coordination polymer in **P5**, which contains a longer Cu–Cl bond in the $[Cu^{II}Cl(tpmtm)]$ moiety (2.3144(9) Å), is assumed to adopt two-dimensional sheet rather than one-dimensional chain structure.

There are some relationships between the numbers of the outer coordination sites on the $[Cu^{II}Cl(tpmtm)]$ moieties and structures of the coordination polymers. Participation in the coordination of two, three, or four outer coordination sites on the tripodal complex afforded the one-dimensional chain, two-dimensional sheet, or three-dimensional structures, respectively (Tables 4 and 5).

The τ value for the geometry around the copper centers of the $[Cu^{II}Cl(tpmtm)]$ moieties in the coordination polymers vary from 0.48 to 0.94 meaning that the copper center of the $[Cu^{II}Cl(tpmtm)]$ moiety can change its coordination geometry between distorted square pyramidal and trigonal bipyramidal depending on the situation. This structural flexibility of the $[Cu^{II}Cl(tpmtm)]$ moiety gives advantage for utilization of the complex as a bridging ligand to make coordination polymers. The polymers with outer coordination with all of the three pyrimidine units, **P6**-cage shape and **P7**, reveal the τ values close to 1.0 meaning less distortion from trigonal bipyramidal structure. On the other hand, the τ values are relatively smaller, which represent the square pyramidal distortion from the ideal trigonal bipyramidal structure, for the one-dimensional coordination polymers with outer coordination using two of three pyrimidine units in the $[Cu^{II}Cl(tpmtm)]$ moieties (0.51, 0.54, and 0.61 for **P1**; 0.68 for **P3**; 0.64 and 0.75 for **P4**; 0.64 for **P6**-linear) except for **P2** (0.86) which contains discrete molecules of $[Cu^{II}Cl(tpmtm)]$. The two-dimensional coordination polymer **P5** with outer sphere coordination using two of the three pyrimidine units also shows smaller τ value (0.48). These results imply that unsymmetrical outer sphere coordination of the pyrimidine units causes the distortion toward square pyramidal structure from trigonal bipyramidal. Furthermore, crystal packing is also an important factor to determine the distortion of the $[Cu^{II}Cl(tpmtm)]$ moiety, because large moieties such as discrete molecules of $[Cu^{II}Cl(tpmtm)]$ in **P2** make the distortion of the $[Cu^{II}Cl(tpmtm)]$ moiety in the coordination polymers smaller. This structural flexibility between trigonal bipyramidal and square pyramidal of the [CuCl(tpmtm)] unit possibly affects its electronic structure and magnetic properties of the resulting coordination polymer and it means that the unit

Table 4. Relationship between the Number of Outer Coordination Sites Used and Dimension of Coordination Polymers, and Selected Bond Distances (Å), Angles (°), and τ Parameters of [CuCl(tpmtm)] Units for **P1–P4**

	P1			**P2**		**P3**	**P4**	
	Cu(1)	Cu(2)	Cu(5)	Cu(1)	Cu(3)	Cu(1)	Cu(1)	Cu(2)
Num. of outer coord sites used	2 (2N)	2 (2N)	2 (2N)	2 (2N)	0	2 (2N)	2(3) (2N (+1S))	2(3) (2N (+1S))
Dimension of polymer	1D	1D	1D	1D	discrete molecule	1D	1D	1D
Contained $[Cu_nCl_m]$ unit	$[Cu_2Cl_2]$	$[Cu_2Cl_2]$	$[Cu_2Cl_2]$	$[Cu_2Cl_2]$		$[Cu_2Cl_2Cu(CH_3CN)_2]$	$[Cu_2Cl_2Cu(CH_3CN)_2]$	
Cu–C	2.040(10)	2.032(9)	2.051(10)	2.02(2)	2.03(2)	2.032(4)	2.025(5)	2.033(5)
Cu–Cl	2.290(2)	2.293(2)	2.312(3)	2.282(6)	2.291(7)	2.2908(13)	2.2796(16)	2.2790(17)
Cu–N	2.062(9)	2.019(9)	2.037(10)	2.058(17)	2.095(15)	2.168(4)	2.078(4)	2.106(4)
	2.067(8)	2.078(8)	2.083(8)	2.107(12)	2.096(14)	2.090(4)	2.180(4)	2.165(5)
	2.174(9)	2.181(9)	2.182(10)	2.108(15)	2.069(15)	2.037(4)	2.054(4)	2.040(4)
C–Cu–Cl	178.3(2)	177.7(3)	179.3(3)	176.9(4)	177.9(5)	176.25(14)	176.61(16)	175.21(16)
N–Cu–N	146.0(3)	147.1(3)	142.6(3)	124.0(5)	113.2(5)	98.44(16)	100.35(18)	97.49(18)
	101.4(3)	107.3(3)	108.2(3)	125.2(6)	122.4(6)	124.25(16)	138.29(18)	130.35(18)
	111.4(3)	104.1(3)	108.5(3)	109.3(5)	122.8(6)	135.62(17)	119.41(18)	130.53(19)
τ	0.54	0.51	0.61	0.86	0.92	0.68	0.64	0.75

Table 5. Relationship between the Number of Outer Coordination Sites Used and Dimension of Coordination Polymers, and Selected Bond Distances (Å), Angles (°), and τ Parameters of [CuCl(tpmtm)] Units for **P5–P7**

	P5	**P6**		**P7**
	Cu(1)	Cu(2)	Cu(1)	Cu(1)
Num. of outer coord sites used	3 (2N1Cl)	2 (2N)	3 (3N)	4 (3N1Cl)
Dimension of polymer	2D	1D	2D	3D
Contained $[Cu_nCl_m]$ unit	Linear $[Cu_4Cl_6]$	Linear $[Cu_3Cl_4]$	Cage-shaped $[Cu_4Cl_6]$	$[Cu_2Cl_2]$
Cu–C	2.056(3)	2.057(5)	2.052(4)	2.021(4)
Cu–Cl	2.3144(9)	2.2884(16)	2.2928(13)	2.3235(13)
Cu–N	2.148(2)	2.065(4)	2.076(4)	2.097(5)
	2.042(2)	2.138(3)	2.092(4)	2.069(4)
	2.068(2)	2.034(5)	2.103(4)	2.109(6)
C–Cu–Cl	177.12(9)	179.34(13)	178.39(15)	178.97(18)
N–Cu–N	109.28(11)	106.82(16)	120.31(16)	117.2(2)
	101.54(10)	140.98(17)	122.27(17)	114.46(19)
	148.22(11)	111.73(17)	116.36(16)	126.3(2)
τ	0.48	0.64	0.94	0.88

is a possible candidate for electronically tunable building blocks.

Conclusion

Redox active tripodal complexes with tpmtm ligand which contains three pyrimidine groups, $[Cu^{II}L(tpmtm)]^{n+}$ (L = CH_3CN, Cl, and OH), were synthesized. The chloro complex, $[Cu^{II}Cl(tpmtm)]$, was used as a bridging ligand to prepare coordination polymers. In the obtained polymers, the complex worked as bidentate, tridentate, or tetradentate bridging ligand with pseudo-tetrahedral geometry to form one-, two-, or three-dimensional structures, respectively. The structural flexibility of the chloro tpmtm complex as a building block stabilizes the versatile structures of the $[Cu_nCl_m]$ moieties in the coordination polymers. Complicated equilibria derived from the amount of CuCl, $CuCl_2$, and $[Cu(CH_3CN)_4]^+$, including the redox equilibria in the presence of oxidizing agents such as $(p\text{-}BrC_6H_4)_3NPF_6$, also lead to formation of various $[Cu_nCl_m]$ moieties with the copper(I) and copper(II) mixed-valence states. The preparation of coordination polymer containing the tpmtm copper(III) complex moieties and/or transition-metal moieties instead of copper chlorides is under investigation.

Experimental

Materials. All chemicals were purchased from Aldrich, Nacalai Tesque, and Wako Pure Chemicals. All reagents and solvents were used without further purification except when otherwise mentioned. Anhydrous solvents were purchased from Nacalai Tesque.

General Procedure. An MBRAUN UNIlab OP7 globebox system was used for rigorously anhydrous conditions under an argon atmosphere. IR spectra were recorded on JASCO FT/IR-420 or JASCO FT/IR-6200 type A spectrophotometers in the range of 4000–400 or 4000–550 cm^{-1}, respectively. Electronic spectra were recorded on JASCO V-570 and Shimadzu Multispec-1500 spectrophotometers. Electrochemical measurements were performed with a BAS CV-50W voltammetric analyzer. Cyclic voltammograms were recorded at 25 °C with platinum disk working (ϕ 1.6 mm), Ag/Ag^+ reference, and platinum counter electrodes in dichloromethane with 0.1 M *n*-Bu_4NPF_6 supporting electrolyte. All data were referred to an internal Fc/Fc^+ couple, of which the redox potential was standardized as 0.400 V vs. SHE. Elemental analyses were performed by the Analytical Research Service Center at Osaka City University on FISONS Instrument EA108 or Perkin-Elmer 240C elemental analyzers.

Synthesis of Tris(2-pyrimidylthio)methane (tpmtmH). An aqueous solution (50 mL) of sodium hydroxide (1.20 g, 30.0 mmol) was added to a solution of 2-sulfanylpyrimidine (2.6 g, 23.2 mmol) and iodoform (2.00 g, 5.08 mmol) in 250 mL of acetonitrile. After the mixture was refluxed under an argon atmosphere for 10 h, the solvent of the reaction mixture was evaporated to dryness and then the residue was extracted with 200 mL of dichloromethane. After insoluble materials were filtered off, the solvent of the extract was removed. The crude product was purified by silica gel column chromatography using CH_2Cl_2/CH_3CN (8:1) as an eluent. The solvent of the second fraction was removed to give a colorless powder, which was recrystallized from CH_2Cl_2/diethyl ether to afford colorless crystals of tpmtmH within a week (0.890 g, 50%). Anal. Calcd for $C_{13}H_{10}N_6S_3$: C, 45.07; H, 2.91; N, 24.26%. Found: C, 45.02; H, 2.82; N, 24.08%. ^1H NMR ($CDCl_3$): δ 8.560 (d, $^3J_{H-H} = 4.8$ Hz, 6H, 4-pm, 6-pm (pm: pyrimidyl)), 7.821 (s, 1H, CH), 6.999 (t, $^3J_{H-H} = 4.2$ Hz, 3H, 5-pm). ^{13}C NMR ($CDCl_3$): δ 170.64 (2-pm), 157.38 (4-pm, 6-pm), 116.92 (5-pm), 49.48 (CH). IR (nujor; cm^{-1}): 2924(s), 1550(s), 1426(m), 1378(s), 1265(w), 1182(s), 1158(s), 1067(w), 984(w), 803(s), 771(s), 748(s), 667(m), 630(s), 477(w), 413(m).

Synthesis of [Cu(CH_3CN)(tpmtm)](PF_6) (1). A mixture of tpmtmH (0.85 g, 2.45 mmol) and triethylamine (0.40 mL, 2.5 mmol) in a mixed solvent of dichloromethane and acetonitrile (10:1) (200 mL) was added to a solution of [Cu(CH_3CN)$_4$](PF_6) (0.80 g, 2.15 mmol) in the mixed solvent (100 mL). After the mixture was stirred for 2 h, the purple reaction mixture was filtered to remove insoluble solids. The solvent of the filtrate was evaporated to dryness. The residue was dissolved in acetonitrile and diethyl ether was slowly added to the solution to give purple solids of **1** (0.90 g, 1.5 mmol, 70%).

Synthesis of [Cu(OH)(tpmtm)](Et_3NH)(PF_6) (2). A solution of tpmtmH (0.053 g, 0.15 mmol) and triethylamine (0.07 mL, 0.42 mmol) in 10 mL of dichloromethane was added to a solution of [Cu(CH_3CN)$_4$](PF_6) (0.072 g, 0.19 mmol) in 20 mL of dichloromethane. While the yellow mixture was stirred for 4.5 h at room temperature, the reaction mixture turned black. After insoluble solids were removed by filtration, diethyl ether was added to the filtrate to give crystals of **2** (0.020 g, 0.03 mmol, 20%). IR (KBr; cm^{-1}): 3413(w), 2986(w), 2954(w), 2921(w), 2441(w), 1570(m), 1557(m), 1475(w), 1431(w), 1380(s), 1189(m), 839(s), 764(w), 753(w), 671(w), 643(w), 558(m).

Synthesis of [CuCl(tpmtm)] (3). A solution of tpmtmH (0.85 g, 2.45 mmol) and triethylamine (0.4 mL) in 2.5 mL of a mixed solvent of dichloromethane and acetonitrile (10:1) was added to a solution of [Cu(CH_3CN)$_4$](PF_6) (0.80 g, 2.15 mmol) in the mixed solvent. After stirring for 2 h, the purple reaction mixture was filtered to remove insoluble materials. The solvent of the filtrate was evaporated to dryness. The residue was dissolved in acetone and then water (20 mL) was added. After removing acetone in vacuo, an aqueous solution of NaCl (0.143 g, 2.45 mmol) was added to the solution. The mixture was extracted with dichloromethane (ca. 100 mL) three times. The solvent of the combined purple organic extract evaporated to dryness. The residue was crystallized from dichloromethane/hexane to give purple crystals of the complex (0.32 g, 0.72 mmol, 33%). Anal. Calcd for $C_{13}H_9ClCuN_6S_3$: C, 35.13; H, 2.04; N, 18.91%. Found: C, 35.12; H, 2.21; N, 18.72%. IR (KRS; cm^{-1}): 3058(w), 1565(m), 1544(s), 1369(s), 1249(m), 1182(s), 1095(w), 1072(w), 825(w), 802(m), 748(s), 657(m), 642(s).

Preparation of [{CuCl(tpmtm)}$_2$(Cu_2Cl_2)]$_n$·2*n*$C_4H_8O_2$ (P1). [CuCl(tpmtm)] (**3**) (0.020 g, 0.045 mmol), CuCl (0.0045 g, 0.045 mmol), and KPF_6 (0.0042 g, 0.023 mmol) were dissolved in 1,4-dioxane (5 mL). After stirring for 3 days, insoluble solids were filtered off. Slow diffusion of hexane into the filtrate afforded some crystals of **P1** ($\leq$2%). IR (KBr; cm^{-1}): 3060(w), 2956(w), 2852(w), 1561(s), 1377(s), 1253(m), 1189(m), 1117(m), 870(m), 812(w), 754(m).

Preparation of [{CuCl(tpmtm)}$_2$(Cu_2Cl_2)]$_n$·*n*[CuCl(tpmtm)] (P2). A mixture of [CuCl(tpmtm)] (**3**) (0.020 g, 0.045 mmol), $CuCl_2$ (0.0061 g, 0.045 mmol), and [Cu(CH_3CN)$_4$](PF_6) (0.0086 g, 0.023 mmol) in acetonitrile (5 mL) was stirred for 10 h. Slow evaporation of the solvent of the reaction mixture gave some purple crystals of **P2** ($\leq$2%). IR (KBr; cm^{-1}): 2923(m), 2851(w), 1561(s), 1331(s), 1387(s), 1379(s), 1251(w), 1185(m), 822(w), 811(w), 797(w), 755(m), 643(w).

Preparation of [{CuCl(tpmtm)}$_2$(Cu_2Cl_2{Cu(CH_3CN)$_2$})]$_n$(PF_6)$_n$·*n*PhMe·*n*CH_3CN (P3). $CuCl_2$ (0.005 g, 0.037 mmol) was added into a mixture of [CuCl(tpmtm)] (**3**) (0.025 g, 0.056 mmol) and [Cu(CH_3CN)$_4$](PF_6) (0.0063 g, 0.017 mmol) in acetonitrile (10 mL). After stirring for 10 h, insoluble solids were filtered off. Removal of the solvent in vacuo gave black powder, which was re-dissolved in dichloromethane (5 mL). After removal of insoluble solids by filtration, the solvent was removed. Slow diffusion of toluene (20 mL) into a solution of the residue in acetonitrile (2 mL) afforded purple crystals of **P3** within 3 days (0.005 g, 11%). IR (KBr; cm^{-1}): 2363(w), 1563(s), 1375(s), 1257(w), 1189(m), 1106(m), 836(s), 753(s), 590(w), 557(m).

Preparation of [{CuCl(tpmtm)}$_2$(Cu_2Cl_2{Cu(CH_3CN)$_2$})]$_n$(PF_6)$_n$·1.3*n*Et_2O·0.6*n*CH_3CN (P4). A solution of [CuCl-

Table 6. Crystallographic Data and Structure Refinement Details for **1**, **2**, and **3**

	1	**2**	**3**
Formula	$C_{15}H_{12}CuF_6N_7PS_3$	$C_{19}H_{26}CuF_6N_7OPS_3$	$C_{13}H_9ClCuN_6S_3$
M_r	595.00	673.15	444.43
Temp/K	193(1)	193(1)	193(1)
Radiation used, λ/Å	Mo Kα, 0.7107	Mo Kα, 0.7107	Mo Kα, 0.7107
Crystal description	purple, block	green, platelet	purple, block
Crystal size/mm^3	0.2 × 0.2 × 0.2	0.4 × 0.2 × 0.03	0.35 × 0.3 × 0.1
Crystal system	monoclinic	monoclinic	orthorhombic
Space group	$P2_1/c$	$P2_1/c$	$Pbca$
a/Å	14.097(11)	16.679(4)	8.8469(13)
b/Å	12.247(9)	9.519(2)	14.621(2)
c/Å	13.833(11)	17.557(4)	25.027(4)
α/°	90	90	90
β/°	109.892(17)	102.575(5)	90
γ/°	90	90	90
V/Å	2246(3)	2720.5(10)	3237.1(8)
Z	4	4	8
F(000)	1188	1372	1784
ρ_{calcd}/g cm^{-3}	1.760	1.643	1.824
μ/mm^{-1}	1.391	1.161	1.909
Total reflections	20834	25650	28332
Unique reflections	5073	6104	3674
R(int)	0.142	0.075	0.033
Scan range θ/°	27.48	27.48	27.48
Completeness to θ_{max}/%	0.986	0.978	0.988
Index ranges	$-18 \le h \le 18$	$-21 \le h \le 19$	$-11 \le h \le 10$
	$-15 \le k \le 15$	$-9 \le k \le 12$	$-15 \le k \le 18$
	$-14 \le l \le 17$	$-22 \le l \le 18$	$-32 \le l \le 32$
Data/restrains/parameters	5073/364	6104/379	3674/226
$R1$ [$I > 2\sigma(I)$], $wR2$ (all data)	0.0886/0.2477	0.0525/0.0963	0.0270/0.0650
Goodness of fit on F^2	1.006	1.043	1.038
Max./min. e$^-$ densities/eÅ^{-3}	3.61/−1.51	1.55/−1.14	0.8/−0.41
Min./max. T factors	0.393/0.757	0.797/0.966	0.520/0.826

(tpmtm)] (**3**) (0.020 g, 0.045 mmol), CuCl (0.0045 g, 0.045 mmol), and KPF_6 (0.0042 g, 0.023 mmol) was dissolved in acetonitrile (5 mL). After the mixture was stirred for 3 days, insoluble solids were removed by filtration. Slow diffusion of diethyl ether afforded some crystals of **P4** (≤2%). IR (KBr; cm^{-1}): 3065(w), 2970(w), 2919(w), 1619(w), 1566(s), 1380(s), 1256(w), 1189(m), 1106(w), 848(s), 752(m), 558(m), 473(s).

Preparation of [{CuCl(tpmtm)}$_2$(Cu$_4$Cl$_6$)]$_n$·4*n*CH$_2$Cl$_2$ (P5). Preparation of **P5** was performed in a globe box. (p-BrC$_6$H$_4$)$_3$NPF$_6$ (0.007 g, 0.01 mmol) was added to a solution of [CuCl(tpmtm)] (**3**) (0.010 g, 0.022 mmol) in dichloromethane (2 mL). CuCl (0.005 g, 0.05 mmol) was dissolved in a solution of Bu_4NCl (0.012 g, 0.043 mmol) in dichloromethane (1 mL) and the solution was added to the solution containing **3**. The mixture was allowed to stand for 2 weeks affording crystals of **P5** (0.0054 g, 36%). IR (KRS; cm^{-1}): 3077(w), 1567(m), 1556(m), 1376(s), 1261(m), 1191(m), 809(m), 754(m), 730(s), 701(m), 669(w), 644(w), 622(w).

Preparation of [{CuCl(tpmtm)}$_2$(Cu$_3$Cl$_4$)]$_n$[{CuCl(tpmtm)}$_2$(Cu$_4$Cl$_6$)]$_n$·4*n*CH$_3$CN (P6). A solution of $CuCl_2$ (0.003 g, 0.02 mmol) in acetonitrile (1 mL) was added to a solution of [CuCl(tpmtm)] (**3**) (0.010 g, 0.022 mmol) in acetonitrile (1 mL). After 30 s, $AgPF_6$ (0.003 g, 0.01 mmol) in acetonitrile (1 mL) was added to the reaction mixture. After stirring for 30 min, insoluble solids were removed by filtration using a glass filter to give a purple filtrate, which was concentrated to 2 mL. Slow diffusion of diethyl ether afforded some crystals of **P6** after 3 weeks (≤2%).

Preparation of [{CuCl(tpmtm)}(Cu$_2$Cl$_2$)]$_n$·*n*CH$_2$Cl$_2$ (P7). A mixture of [CuCl(tpmtm)] (**3**) (0.010 g, 0.022 mmol) and [Cu(CH$_3$CN)$_4$](PF$_6$) (0.0083 g, 0.022 mmol) in dichloromethane (2 mL) was allowed to stand for 2 weeks to give dark purple crystals of **P7** (0.0072 g, 50%). IR (KRS; cm^{-1}): 3066(w), 1562(s), 1378(s), 1255(s), 1187(m), 835(s), 804(s), 750(s), 728(s), 678(m), 661(w), 559(m).

X-ray Crystallography. Each single crystal was mounted on a glass fiber. Diffraction data were collected on an AFC7/CCD Mercury diffractometer using a rotation method with 0.15 for **P1**, 0.25 for **P2**, 0.3 for **P4**, and 0.5 frame widths for the others and with exposure times per frame of 15 s for **P1**, 8 s for **P2**, 5 s for **P5**, and 10 s for the others. The data were integrated, scaled, sorted, and averaged using the CrystalClear[14] software. Absorption corrections were applied using the Coppens numerical method for **2**, **3**, and **P2** and the multiscan method for the others. The structures were solved using SHELX97[15] for **1**, **P1**, and **P4** and SIR97[16] for the others and refined with

Table 7. Crystallographic Data and Structure Refinement Details for **P1**, **P2**, **P3**, **P4**, **P5**, **P6**, and **P7**

	P1	**P2**	**P3**	**P4**	**P5**	**P6**	**P7**
Formula	$C_{57}H_{63}Cl_6Cu_6N_{18}O_9S_9$	$C_{26}H_{18}Cl_3Cu_3N_{12}S_6$	$C_{39}H_{41}Cl_4Cu_5F_6N_{14.5}PS_6$	$C_{36.2}H_{21}Cl_4Cu_5F_6N_{14.6}O_{1.3}PS_6$	$C_{15}H_9Cl_8Cu_3N_6S_3$	$C_{30}H_{24}Cl_7Cu_{5.5}N_{14}S_6$	$C_{14}H_{11}Cl_5Cu_3N_6S_3$
M_r	2026.77	987.87	1509.72	1478.13	843.72	1370.65	727.36
Temp/K	193(1)	193(1)	193(1)	193(1)	193(1)	193(1)	193(1)
Radiation used, λ/Å	Mo Kα, 0.7107	Mo Kα, 0.7107	Mo Kα, 0.7107	Mo Kα, 0.7107	Mo Kα, 0.7107	Mo Kα, 0.7107	Mo Kα, 0.7107
Crystal description	purple, prism	purple, chip	brown, prism	black, prism	purple, block	purple, platelet	purple, platelet
Crystal size/mm^3	0.15 × 0.05 × 0.05	0.1 × 0.1 × 0.02	0.3 × 0.3 × 0.2	0.25 × 0.2 × 0.1	0.3 × 0.2 × 0.2	0.25 × 0.2 × 0.1	0.2 × 0.2 × 0.1
Crystal system	triclinic	triclinic	monoclinic	monoclinic	triclinic	triclinic	triclinic
Space group	$P\bar{1}$	$P\bar{1}$	$P2_1/m$	$P2_1/n$	$P\bar{1}$	$P\bar{1}$	$P\bar{1}$
a/Å	11.191(4)	11.354(5)	11.863(3)	14.339(3)	9.4532(16)	11.507(2)	8.437(2)
b/Å	18.547(6)	12.779(5)	21.418(4)	21.390(4)	11.4897(19)	11.8065(19)	11.226(3)
c/Å	19.309(7)	12.983(4)	12.160(2)	19.331(3)	13.012(2)	17.381(3)	13.491(3)
α/°	75.053(10)	69.44(3)	90	90	90.013(4)	87.052(8)	67.040(16)
β/°	85.930(12)	78.87(4)	106.439(5)	91.094(3)	92.552(5)	89.384(8)	80.20(2)
γ/°	77.835(10)	81.47(4)	90	90	98.336(5)	79.463(6)	84.43(2)
V/Å	3785(2)	1723.9(11)	2963.4(9)	5927.9(18)	1396.9(4)	2318.5(7)	1158.7(5)
Z	2	2	2	4	2	2	2
F(000)	2046	984	1509	2915.2	824	1353	714
ρ_{calcd}/g cm^{-3}	1.778	1.903	1.692	1.656	2.006	1.963	2.085
μ/mm^{-1}	2.181	2.472	2.246	2.246	3.271	3.197	3.592
Total reflections	30083	16958	25358	42929	13290	22526	10864
Unique reflections	16633	7479	6524	10465	5953	9928	4909
R(int)	0.092	0.167	0.035	0.037	0.024	0.032	0.037
Scan range θ/°	27.48	27.48	27.53	27.2	27.48	27.48	27.48
Completeness to θ_{max}/%	0.958	0.945	0.931	0.792	0.93	0.935	0.924
Index ranges	$-9 \le h \le 14$	$-13 \le h \le 14$	$-15 \le h \le 15$	$-16 \le h \le 13$	$-12 \le h \le 12$	$-14 \le h \le 13$	$-10 \le h \le 8$
	$-23 \le k \le 24$	$-13 \le k \le 16$	$-23 \le k \le 27$	$-24 \le k \le 24$	$-12 \le k \le 14$	$-15 \le k \le 11$	$-14 \le k \le 14$
	$-25 \le l \le 24$	$-14 \le l \le 16$	$-15 \le l \le 13$	$-16 \le l \le 22$	$-16 \le l \le 16$	$-22 \le l \le 22$	$-17 \le l \le 15$
Data/restrains/parameters	16633/965	7479/432	6524/371	10465/802	5953/353	9928/566	4909/281
$R1$ [$I > 2\sigma(I)$], $wR2$ (all data)	0.1210/0.2292	0.1746/0.3301	0.0632/0.1615	0.0661/0.1361	0.0389/0.0981	0.0485/0.1070	0.0592/0.1413
Goodness of fit on F^2	1.210	1.228	1.043	1.019	1.026	1.002	1.091
Max./min. e$^-$ densities/eÅ^{-3}	1.30/−1.10	1.71/−1.09	1.08/−1.66	1.04/−2.04	1.17/−1.21	1.32/−0.81	0.95/−0.97
Min./max. T factors	0.490/0.897	0.805/0.952	0.539/0.638	0.617/0.799	0.377/0.520	0.568/0.726	0.453/0.698

CRYSTALS[17] for **1**, **2**, and **3** and SHELXL97[15] for the others using CrystalStructure 3.8[18] software. Crystallographic data are summarized in Tables 6 and 7. Disordered F atoms of PF_6 and the O atom in **2**, three pyrimidine carbon atoms in **P2** and a part of disordered solvent molecules in **P4** were refined isotropically. All the other non-hydrogen atoms were refined anisotropically. All hydrogen atoms except for **P5** were located on the calculated positions and refined as ridding models. Hydrogen atoms in **P5** were found in difference Fourier maps and refined isotropically. Although the data for **P2** and **P4** were preliminary due to the bad quality of the crystals, the framework of the coordination polymers clearly appeared, and the data were included for discussion.

Crystallographic data have been deposited with the Cambridge Crystallographic Data Center: Deposition numbers CCDC-765631–765640 for compounds **1**–**3** and **P1**–**P7**, respectively. Copies of the data can be obtained free of charge via http://www.ccdc.cam.ac.uk/conts/retrieving.html (or from the Cambridge Crystallographic Centre, 12, Union Road, Cambridge, CB2 1EZ, U.K.; Fax: +44 1223 336033; e-mail: deposit@ccdc.cam.ac.uk).

References

1 K. A. Cychosz, A. G. Wong-Foy, A. J. Matzger, *J. Am. Chem. Soc.* **2009**, *131*, 14538; C. R. Samanamu, M. M. Olmstead, J.-L. Montchamp, A. F. Richards, *Inorg. Chem.* **2008**, *47*, 3879; K. Koh, A. G. Wong-Foy, A. J. Matzger, *Angew. Chem., Int. Ed.* **2008**, *47*, 677; E. R. Parnham, R. E. Morris, *Acc. Chem. Res.* **2007**, *40*, 1005; K.-Z. Shao, Y.-H. Zhao, Y. Xing, Y.-Q. Lan, X.-L. Wang, Z.-M. Su, R.-S. Wang, *Cryst. Growth Des.* **2008**, *8*, 2986.

2 S. Delgado, P. J. S. Miguel, J. L. Priego, R. Jiménez-Aparicio, C. J. Gómez-García, F. Zamora, *Inorg. Chem.* **2008**, *47*, 9128; D. Sun, G.-G. Luo, Q.-J. Xu, N. Zhang, Y.-C. Jin, H.-X. Zhao, L.-R. Lin, R.-B. Huang, L.-S. Zheng, *Inorg. Chem. Commun.* **2009**, *12*, 782; J.-B. Liu, H.-H. Li, Z.-R. Chen, J.-B. Li, X.-B. Chen, C.-C. Huang, *J. Cluster Sci.* **2009**, *20*, 515; V. A. Montes, G. V. Zyryanov, E. Danilov, N. Agarwal, M. A. Palacios, P. Anzenbacher, Jr., *J. Am. Chem. Soc.* **2009**, *131*, 1787; X.-B. Chen, H.-H. Li, Z.-R. Chen, J.-B. Liu, J.-B. Li, H.-J. Dong, Y.-L. Wu, *J. Cluster Sci.* **2009**, *20*, 611; K. L. Yao, J. Q. Zhang, Z. L. Liu, G. Y. Gao, Y. L. Li, D. Xi, Q. Ning, *J. Magn. Magn. Mater.* **2008**, *320*, 458; X.-C. Zhang, Y.-H. Chen, B. Liu, *Inorg. Chem. Commun.* **2008**, *11*, 446.

3 S. Bureekaew, S. Horike, M. Higuchi, M. Mizuno, T. Kawamura, D. Tanaka, N. Yanai, S. Kitagawa, *Nat. Mater.* **2009**, *8*, 831; S. Morikawa, T. Yamada, H. Kitagawa, *Chem. Lett.* **2009**, *38*, 654; T. Yamada, M. Sadakiyo, H. Kitagawa, *J. Am. Chem. Soc.* **2009**, *131*, 3144; K. Kanaizuka, R. Haruki, O. Sakata, M. Yoshimoto, Y. Akita, H. Kitagawa, *J. Am. Chem. Soc.* **2008**, *130*, 15778; M. Fujishima, S. Kanda, T. Mitani, H. Kitagawa, *Synth. Met.* **2001**, *119*, 485.

4 S. Kitagawa, S. Noro, *Comprehensive Coordination Chemistry II*, ed. by J. A. McCleverty, T. J. Meyer, Elsevier Ltd., **2003**, Vol. 7, p. 231. doi:10.1016/B0-08-043748-6/06192-2

5 I. Kinoshita, L. J. Wright, S. Kubo, K. Kimura, A. Sakata, T. Yano, R. Miyamoto, T. Nishioka, K. Isobe, *Dalton Trans.* **2003**, 1993.

6 R. Miyamoto, R. Santo, T. Matsushita, T. Nishioka, A. Ichimura, Y. Teki, I. Kinoshita, *Dalton Trans.* **2005**, 3179.

7 R. Santo, R. Miyamoto, R. Tanaka, T. Nishioka, K. Sato, K. Toyota, M. Obata, S. Yano, I. Kinoshita, A. Ichimura, T. Takui, *Angew. Chem., Int. Ed.* **2006**, *45*, 7611.

8 R. Miyamoto, R. T. Hamazawa, M. Hirotsu, T. Nishioka, I. Kinoshita, L. J. Wright, *Chem. Commun.* **2005**, 4047.

9 I. Kinoshita, H. Hashimoto, T. Nishioka, R. Miyamoto, N. Kuwamura, Y. Yoshida, *Photosynth. Res.* **2008**, *95*, 363.

10 Y. Yoshida, R. Miyamoto, T. Nishioka, H. Hashimoto, I. Kinoshita, *Chem. Lett.* **2009**, *38*, 366.

11 A. W. Addison, T. N. Rao, J. Reedijk, J. van Rijn, G. C. Verschoor, *J. Chem. Soc., Dalton Trans.* **1984**, 1349.

12 W. Hiller, *Acta Crystallogr., Sect. C* **1986**, *42*, 149.

13 J. C. Dyason, L. M. Engelhardt, P. C. Healy, C. Pakawatchai, A. H. White, *Inorg. Chem.* **1985**, *24*, 1950.

14 *CrystalClear*, Rigaku Corporation, **1999**; *CrystalClear Software User's Guide*, Molecular Structure Corporation, **2000**; J. W. Pflugrath, *Acta Crystallogr., Sect. D* **1999**, *55*, 1718.

15 G. M. Sheldrick, *SHELX-97, Program for Crystal Structure Refinement*, University of Göttingen, Göttingen, Germany, **1997**.

16 A. Altomare, M. C. Burla, M. Camalli, G. Cascarano, C. Giacovazzo, A. Guagliardi, A. G. G. Moliterni, G. Polidori, R. Spagna, *J. Appl. Crystallogr.* **1999**, *32*, 115.

17 J. R. Carruthers, J. S. Rollett, P. W. Betteridge, D. Kinna, L. Pearce, A. Larsen, E. Gabe, *CRYSTALS Issue 11*, Chemical Crystallography Laboratory, Oxford, UK, **1999**.

18 *CrystalStructure 3.8, Crystal Structure Analysis Package*, Rigaku and Rigaku Americas **2000–2007**.